Pentamethylcyclopentadienyl Ru Complexes V*. Electrochemistry of Cp*Ru Halide and Donor Ligand Complexes

U. KOELLE** and J. KOSSAKOWSKI

Institute for Inorganic Chemistry, Technical University of Aachen, D-5100 Aachen (F.R.G.)

(Received April 17, 1989)

Abstract

The redox chemistry of three types of Cp*Ru complexes, $[Cp^*Ru(III)X_2]_2$, $Cp^*Ru(III)LX_2$ and $Cp^*Ru(II)L_2X$, X = Cl, Br, I; L = phosphine, diene, bipyridine, was investigated by cyclic voltammetry. The Ru(II) complexes are oxidized reversibly to Ru(III). Complexes $Cp^*Ru(III)LX_2$ undergo irreversible reduction with electron transfer initiated loss of the anionic ligand X and stabilization by addition of L. Reoxidation to Ru(III) occurs anodic of the initial Ru(III)/Ru(II) potential. Complexes $[Cp^*Ru(III)X_2]_2$ show complex redox behavior dependent on the solvent and the supporting electrolyte anion.

Introduction

Introduction of the organometallic Ru(III) halide $[Cp^*RuCl_2]_2$ in 1984 by Bercaw *et al.* and by Suzuki and coworkers [2] added to the traditional complexes of the type $CpRuL_2X$ [3] those of Cp*Ru(III) [4] and Cp*Ru(IV) [5]. A variety of redox reactions encountered among these types such as oxidation to Cp*Ru(IV) complexes by halogens [5] or the ready reduction of Cp*Ru(IV) to Cp*Ru(III) [5] and of Cp*Ru(III) to Cp*Ru(II) complexes by alcohols in the presence of phosphine ligands [2] raise the question as to what are the redox potentials of the Cp*Ru moiety between given oxidation states as a function of ligands L and X.

Ru complexes of various types are used in catalytic redox reactions such as oxidation of alcohols to carbonyl compounds and carboxylic acids [6] and the reduction of molecular oxygen or the oxidation of water as the anodic part of light driven water splitting cycles [7].

Whereas the redox chemistry of Ru coordination compounds is well documented [8] information on redox reactions of organometallic Ru complexes is considerably more sparse and is largely confined to some carbonyls [9] as well as Cp- and arene sandwich complexes [10]. The large body of studies on iron complexes $Cp(^*)FeL_2X$ has no adequate counterpart in Ru chemistry.

Electrochemical studies should be able to answer the question as to the redox potentials involved as well as the preferred coordination modes of the different oxidation states, since loss or addition of ligands upon electron transfer is easily detected by these methods. Investigations presented below are a first survey of complexes prepared recently in our laboratory [1].

Experimental

The preparation and properties of the complexes investigated is detailed in ref. 1. EG&G/PAR electrochemical equipment as described previously has been used for recording cyclic voltammograms at Pt bead or vitreous carbon electrodes. Rapid scan ($v > 1$ V/s) voltammograms were sampled with a Nicolet 3091 digital storage oscilloscope and transferred to a PC. Software for data treatment (displaying, scaling, smoothing etc.) was developed in our laboratory.

A saturated aqueous calomel electrode (SCE) served as the reference electrode and was calibrated against the ferrocene/ferrocenium couple in the respective solvents. Potentials in the tables are normalized to a ferrocene/ferrocenium potential of 0.4 V versus SCE (addition of 0.4 V, i.e. the potential of the ferrocene/ferrocenium couple versus a SCE in CH_2Cl_2, to the quoted value gives the ferrocene/ferrocenium potential in the respective solvent), potentials quoted in the text and displayed in figures are referred to the SCE potential in the respective solvent. Corrections are +10 mV for acetonitrile, +50 mV for methanol and −145 mV for THF.

Electrolytic reductions were performed on a Hg cathode in an H-type cell divided by a nafion ion exchange membrane. A vitreous carbon electrode immersed into the solution allowed the solution to be monitored by cyclic voltammetry intermittently during electrolysis.

*For Parts III and IV, see ref. 1.

**Author to whom correspondence should be addressed.

0020-1693/89/$3.50

TABLE 1. Electrochemical parameters of complexes of Cp*Ru(II)L_2X in CH_2Cl_2

No.	Compound	$E_{1/2}$ (V)[a]	ΔE (mV)[b]	i_{pc}/i_{pa}[c]	ν (mV/s)
1	Cp*Ru($(PPh_2)_2CH_2$)Cl	0.167	65	1	50
2	(Cp*Ru$(Cl)_2(\mu$-$(PPh_2)_2CH_2)$)	−0.195[d]	70	1	100
		0.337	75	1	100
3	Cp*Ru(bipy)Cl	0.07	73	1	100
4	Cp*Ru(COD)Cl	0.637	65	0.66	100
				0.89	200

[a]Mean of anodic and cathodic peak potential. [b]Separation of anodic and cathodic peak potential. [c]Peak current ratio. [d]Two successive reversible waves, see text.

Results and Discussion

*Complexes Cp*Ru(II)L_2X*

This type is exemplified by compounds **1**–**4** of Table 1. The cyclic voltammograms of these complexes are of the simple reversible or quasireversible type common for an unperturbed one electron transition, cf. Fig. 1 for complex **3**. Electrochemical parameters are given in Table 1.

Starting with the neutral Ru(II) complex a 17-electron monocation with identical coordination is formed according to eqn. (1):

$$Cp^*Ru(II)L_2X \xrightarrow{-e^-} [Cp^*Ru(II)L_2X]^+ \qquad (1)$$

Two successive transitions of equal peak heights and equal peak current ratio (Fig. 2) are observed when the dinuclear bridged phosphine complex **2** is oxidized. The first peak with $E_{1/2} = -0.2$ V is shifted cathodic with respect to the oxidation peak of **1** due to the fact that in **2** only one phosphine ligand per Ru center is present. Thus the PR_3 ligand in **1** and **2** acts as a pronounced acceptor.

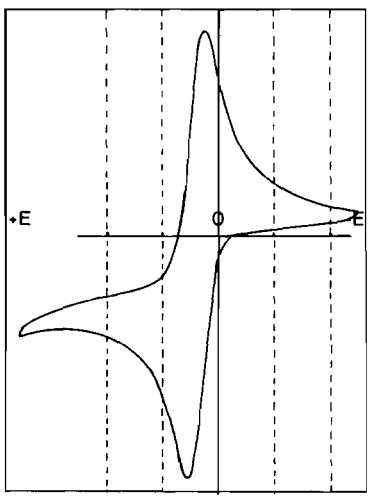

Fig. 1. Repetitive scan cyclic voltammogram of [Cp*Ru(bipyridine)Cl]Cl, 7×10^{-3} M, generated *in situ* from Cp*RuCl_2 and 2,2′-bipyridine in molar ratio 1:1. Supporting electrolyte: CH_2Cl_2/0.1 M TBAH, vitreous carbon electrode, ν = 100 mV/s. For this and subsequent Figures: concentration of electroactive species 2×10^{-3} M if not otherwise specified; solid bar marks begin of sweep; grid spacing 0.2 V.

Peak current ratios are unity for the phosphine and the bipyridine complexes at all scan rates. The dark mauve colored bipyridine derivative **3** has been electrolyzed on the anodic plateau, giving after passage of one F a lighter brown–red colored solution with a cyclic voltammogram shifted only on the current axis. Back electrolysis re-establishes the original cyclic voltammogram. The same brown–red solution, indicative of the formation of the cation 3^+, is formed directly on addition of one molar equivalent of 2,2′-bipyridine to the solution of $[Cp^*RuCl_2]_2$ in CH_2Cl_2. Upon electrolysis on the cathodic plateau the darker color of the Ru(II) complex **3** develops. Thus the bipyridine complexes form a fully reversible pair on the timescale of electrolysis as well.

Peak current ratios markedly deviate from unity for the 1,5-cyclooctadiene complex **4** at scan rates less than 200 mV/s (Fig. 3). At 50 mV/s only a small cathodic peak is found on the reverse scan, showing the cation $[Cp^*Ru(COD)Cl]^+$ to be of

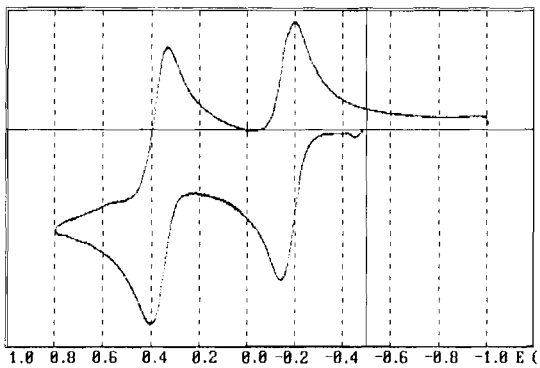

Fig. 2. Cyclic voltammogram of $(Cp^*RuCl)_2(Ph_2P)_2CH_2$ (**2**). Supporting electrolyte: CH_2Cl_2/0.1 M TBAH, vitreous carbon electrode, ν = 100 mV/s.

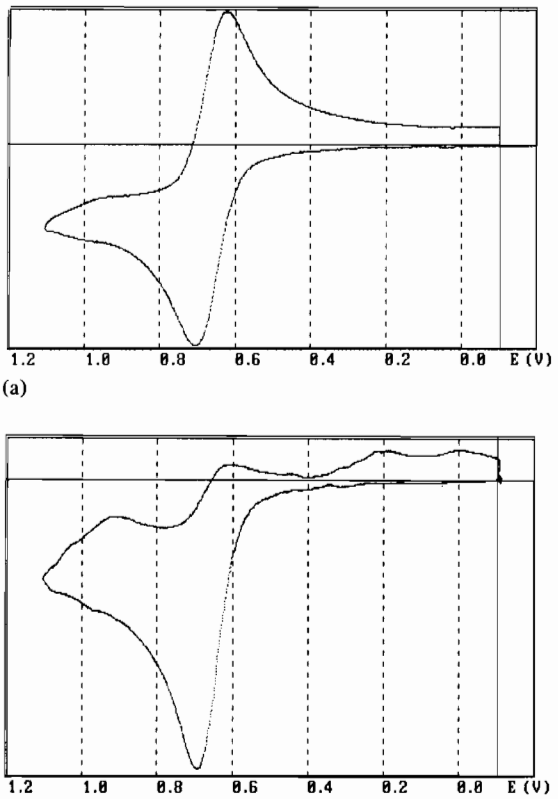

Fig. 3. Cyclic voltammogram of Cp*Ru(1,5-cyclooctadiene)-Cl. Supporting electrolyte: CH_2Cl_2/0.1 M TBAH, Pt bead electrode; (a) $v = 200$ mV/s, (b) $v = 50$ mV/s. Solid bar marks begin of sweep.

limited stability on the cyclovoltammetric time-scale.

*Complexes Cp*Ru(III)LX$_2$*

This type of complex is formed from the halogeno precursors $[Cp^*Ru(III)X_2]_2$ through addition of the appropriate ligand L. In addition to phosphine derivatives described in the literature [5] an acetylacetonate complex **5** and a pyridine adduct **7** of the above type were isolated [1]. For electrochemical investigation in dilute solution was **7** generated *in situ* by addition of excess pyridine to the halogeno complexes. The acetonitrile complex **8** is formed similarly on dissolution of the halogeno compound in acetonitrile.

Most electron transitions encountered in these systems are chemically irreversible and their respective potentials are referred to by peak potentials. Values cited are extracted from a narrow range of sweep rates, mostly 50 or 100 mV/s, to make them more comparable and should be considered as indicating a potential range, where the reduction/oxidation occurs.

Starting with the Ru(III) complex all of the compounds are irreversibly reduced around -0.3 to -0.5 V. In the case of **5** and **6** in the absence of excess ligand reoxidation is indicated by a broad peak of lower intensity at about -0.2 V.

The voltammetric pattern is accounted for by eqn. (2) where loss of halide occurs along with the reduction.

$$Cp^*RuLX_2 \xrightarrow{+e^-} Cp^*RuLX + X^- \quad (2)$$

$$Cp^*RuLX + L \longrightarrow Cp^*RuL_2X \quad (3)$$

$$Cp^*RuL_2X \underset{+e^-}{\overset{-e^-}{\rightleftharpoons}} Cp^*RuL_2X^+ \longrightarrow \text{decomp.} \quad (4)$$

$$Cp^*RuL_2X^+ + X^- \longrightarrow Cp^*RuLX_2 + L \quad (5)$$

Addition of excess PPh_3 to **6** in solution generates a reversible pair with $E_{1/2} = 0.34$ V as the follow up product of a reduction (Fig. 4). This is due obviously to the formation of $Cp^*Ru(PPh_3)_2Cl$, eqn. (3), L = PPh_3, in the cathodic sweep and the persistence of the respective cation $[Cp^*Ru(PPh_3)_2Cl]^+$ in the course of an oxidation, eqn. (4).

In contrast neither **7** in the presence of excess pyridine nor **8** in acetonitrile shows a reversible wave attributable to the $[Cp^*RuL_2X]^{0/+}$ pair. The oxidation wave, though well developed in both cases (Figs. 5 and 6), is displaced anodically occurring

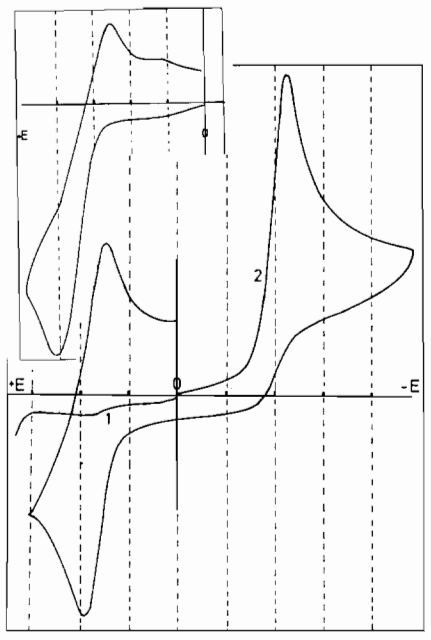

Fig. 4. Cyclic voltammogram of $Cp^*Ru(PPh_3)Cl_2$ (**6**). Supporting electrolyte: CH_2Cl_2/0.1 M TBAH, Pt bead electrode, $v = 100$ mV/s; 1 and inset: pure anodic scan; 2: cathodic–anodic scan after addition of excess PPh_3.

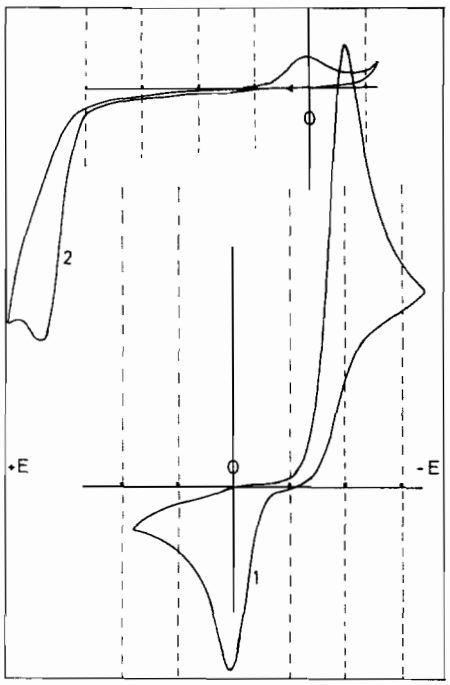

Fig. 5. Repetitive scan cyclic voltammogram of Cp*Ru(pyridine)Cl_2 (7) generated *in situ* by addition of pyridine, 4×10^{-2} M, to Cp*$RuCl_2$, 4×10^{-3} M in CH_2Cl_2. $v = 50$ mV/s. 1: cathodic–anodic scan, 2: pure anodic scan.

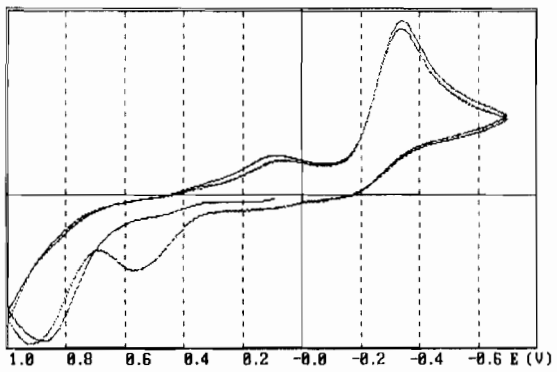

Fig. 6. Repetitive cyclic voltammogram of $[Cp^*RuCl_2]_2$ (9) in acetonitrile/0.1 M TBAH, $v = 50$ mV/s. First anodic scan shows the Ru(III)/Ru(IV) oxidation peak with reduction peak at 0.1 V. Consecutive anodic sweeps show oxidation of intermediately formed Cp*Ru(acetonitrile)$_2$Cl.

near the Ru(III)/Ru(IV) oxidation for 8 (Fig. 6). It is concluded that in these cases species Cp*RuL_2X on reoxidation to the Ru(III) level lose L and either decompose or revert to the starting molecules as indicated in eqns. (4) and (5). Repeated cycling through the +0.35 to −0.6 or the 1.0 to −0.6 V potential range respectively, in either case does not show the formation of any additional electroactive species. Chronoamperograms between the reduction/oxidation limits of 7 are similar to those obtained for a standard (ferrocene) under identical conditions.

Increasing the concentration of pyridine (from 4.2×10^{-2} to 4.2×10^{-1} M) in the cyclic voltammogram of 7 shifts both peaks to more positive potentials in agreement with loss of pyridine in the anodic and uptake in the cathodic sweep.

In the case of 8 no complex has been isolated. The ^1H NMR spectrum of Cp*$RuCl_2$ in acetonitrile [1] is characteristic of a mononuclear species, which on the basis of a negligible conductivity of the solution is assigned the molecular formula Cp*Ru$(NCCH_3)Cl_2$.

Electrolysis of the acetonitrile solution of Cp*RuCl_2 on the plateau of the reduction peak yields a light brown, highly air sentitive solution, which on addition of appropriate ligands, e.g. 1,5-cyclooctadiene or norbornadiene (L_2), forms Cp*RuL_2X and is believed to contain the Ru(II) complexes Cp*Ru$(NCCH_3)_2X$ or $[Cp^*Ru(NCCH_3)_3]^+$. The cyclic voltammogram of the reduced solution is devoid of the reduction peak at −0.38 V and shows the anodic peak at about 0.5 V directly when sweeping in the anodic direction, the cathodic peak at −0.35 V appears as a follow up product.

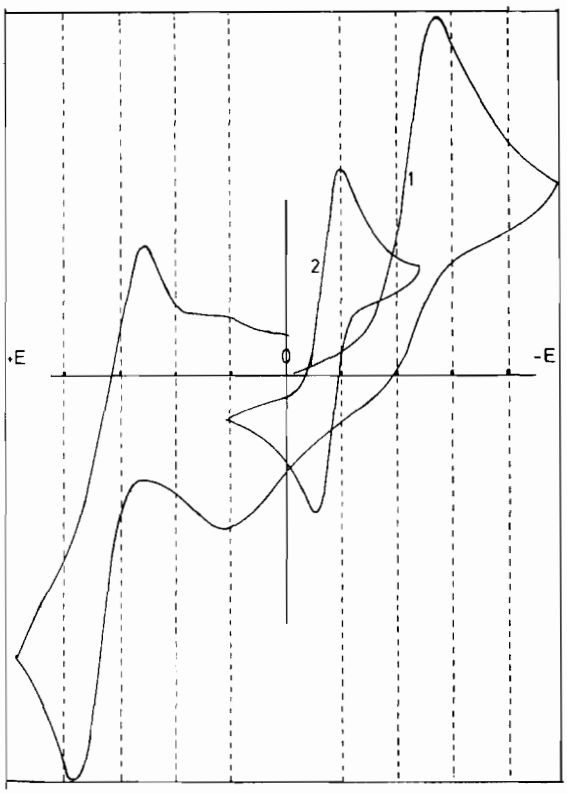

Fig. 7. Cyclic voltammogram of Cp*Ru(acac)Cl (5). Supporting electrolyte: CH_2Cl_2/0.1 M TBAH, Pt bead electrode; 1: extended cathodic–anodic sweep, 2: after addition of excess pyridine, diminished *i* scale sensitivity.

TABLE 2. Electrochemical parameters of complexes $Cp^*Ru(III)LX_2$ in CH_2Cl_2 (CH_3CN for 8)

No.	Compound/System	E_{pc} (V)	E_{pa} (V)	ν (mV/s)	Transition
5	Cp*Ru(acac)Cl	−0.52		100 irrev	Ru(III)/(II)
		0.53[a]	0.78	100	Ru(III)/(IV)
	Cp*Ru(acac)Cl/pyridine	−0.23	−0.125	100	Ru(III)/(II)
6	$Cp^*Ru(PPh_3)Cl_2$	−0.46	−0.22	100 irrev	Ru(III)/(II)
		0.78	0.92	100	Ru(III)/(IV)
	$Cp^*Ru(PPh_3)Cl_2/PPh_3$	0.29	0.39	100 rev	Ru(III)/(II)
7	$[Cp^*RuCl_2]_2$/pyridine	−0.41	0.01	50 irrev	Ru(III)/(II)
	$(4.2 \times 10^{-2}$ M)	−0.38	0.11		
8	$[Cp^*RuCl_2]_2$/acetonitrile	−0.39	0.46	100 irrev	Ru(III)/(II)
		0.24	0.676	100 irrev	Ru(III)/(IV)

[a]Values in a line denote peaks and follow up products belonging either to a cathodic/anodic or to an anodic/cathodic sweep.

Still different is the effect of added pyridine to the acac derivative **5**. A new reversible couple at $E_{1/2} = -0.177$ V (Fig. 7) is now apparent from the beginning indicating the formation of a new Ru(III)/Ru(II) redox pair. As indicated in eqns. (6) and (7) this latter is thought to be $[Cp^*Ru(acac)(pyridine)]^{0/+}$, of the same type as the couples treated in the first section above. A similar reaction leading to a reversible pair at $E_{1/2} = 0.085$ V has been found if excess PPh_3 is added to the solution of 5[†].

$$Cp^*Ru(acac)Cl + \text{pyridine} \longrightarrow [Cp^*Ru(acac)(\text{pyridine})]^+ + Cl^- \quad (6)$$

$$[Cp^*Ru(acac)(\text{pyridine})]^+ \underset{-e^-}{\overset{+e^-}{\rightleftharpoons}} [Cp^*Ru(acac)(\text{pyridine})] \quad (7)$$

An oxidation peak on a pure anodic scan is seen for all complexes 5–8 (Table 2). It is totally irreversible for 7 and 8, where the respective reduction is indicated by a small peak near 0 V and partially reversible for 5 and 6, where reoxidation in CH_2Cl_2 occurs without excessive potential displacement, thus indicating the formation of short lived cations $[Cp^*Ru(acac)Cl]^+$ and $[Cp^*RuPPh_3Cl]^+$ respectively.

Comparison of the cyclic voltammetry of complexes Cp^*RuL_2X and Cp^*RuLX_2 shows that the latter only give rise to a reversible or quasireversible transition if on oxidation a cationic species $[Cp^*RuL_2X]^+$ stable on the electrochemical timescale is generated. This in turn appears to be the case for either chelating ligands L_2 as bipy or acac or for phosphines having donor acceptor properties that stabilize Ru(II) as well as Ru(III). It is not the case for pronounced donor ligands like pyridine or acetonitrile which obviously do not stabilize the cationic form $[Cp^*RuL_2X]^+$ even when they are present in large excess.

$Cp^*Ru(III)$ Halogeno Complexes Cp^*RuX_2

Cyclic voltammetry of these complexes was studied in CH_2Cl_2 and methanol for $[Cp^*RuCl_2]_2$ (**9**), $[Cp^*RuBr_2]_2$ (**10**) and $[Cp^*RuI_2]_2$ (**11**) and in addition in THF for **9**. The cyclovoltammetric patterns in all cases are complicated and require some knowledge of the chemistry of the system for interpretation.

From ^1H NMR spectra, solution molecular weights and conductivity studies it was concluded [1] that **9** exists as the monomeric solvate **9a** in coordinating solvents, e.g. acetonitrile, as the molecular dimeric complex **9b** in CH_2Cl_2 and $CHCl_3$ and as the ionic dimer **9c** in polar ionizing solvents like MeOH.

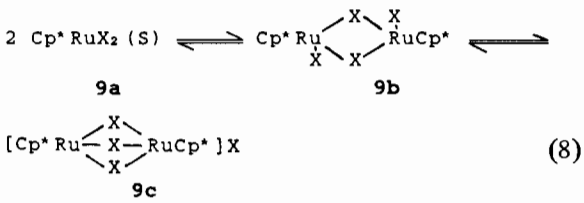

(8)

The cyclic voltammogram in MeOH is the simplest and is discussed first. It consists for all of the halogeno complexes of a two step reversible reduction/oxidation (Fig. 8) at the potentials indicated in Table 3. Both waves are displaced slightly to more negative potentials going along the series Cl, Br, I. The onset of a very intense peak at about 0.7 V, most obvious in the case of **9**, is assigned a catalytic oxidation of the solvent. It will make the subject of a separate investigation.

[†]See 'Note Added in Proof', p. 32.

TABLE 3. Electrochemical parameters of complexes $[Cp^*RuX_2]_2$

No.	Compound	$E_{1/2}{}^1$ [a]	$\Delta E_p{}^1$	$E_{1/2}{}^2$	$\Delta E_p{}^2$	ν (mV/s)
Quasi-irreversible transitions in MeOH						
9	$[Cp^*RuCl_2]_2$	0.145	90	−0.03	100	100
10	$[Cp^*RuBr_2]_2$	0.05	150	−0.095	130	20
11	$[Cp^*RuI_2]_2$	0.04	165	−0.165	170	20

Compound	Solvent	$E_{pc}{}^1$	$E_{pc}{}^2$	$E_{pa}{}^3$	$E_{pa}{}^4$	ν	Transition
Irreversible transitions in CH_2Cl_2 and THF							
$[Cp^*RuCl_2]_2$	CH_2Cl_2	−0.27	−0.355	0.20	0.47	50	Ru(III)/(II)
					0.81		Ru(III)/(IV)
$[Cp^*RuCl_2]_2$/ TEBACl[b]	CH_2Cl_2		−0.47			100	Ru(III)/(II)
			0.608			100	Ru(III)/(IV)
$[Cp^*RuCl_2]_2$	THF	−0.32	−0.47	0.275		50	Ru(III)/(II)
$[Cp^*RuCl_2]_2$/ LiCl	THF	−0.39		−0.005			Ru(III)/(II)
				0.355			Ru(III)/(IV)
$[Cp^*RuBr_2]_2$	CH_2Cl_2	−0.02	−0.39	0.125	0.58	20	Ru(III)/(II)
				0.8			Ru(III)/(IV)
$[Cp^*RuI_2]_2$	CH_2Cl_2	0.12	−0.08	0.16	0.45	20	Ru(III)/(II)
				0.72		20	Ru(III)/(IV)

[a]First and second reduction potential as mean of respective anodic and cathodic peak potential and accompanying peak separation. [b]Triethylbenzylammoniumchloride.

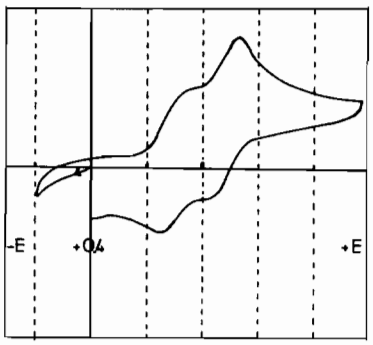

Fig. 8. Cyclic voltammogram of $[Cp^*RuCl_2]_2$ (**9**) in MeOH/ 0.1 M TBAH; ν = 100 mV/s.

The two step reversible reduction, eqn. (9), is in accord with chemical findings, in particular with the formation of the mixed valence dimer **13** upon chemical reduction of **9** [1].

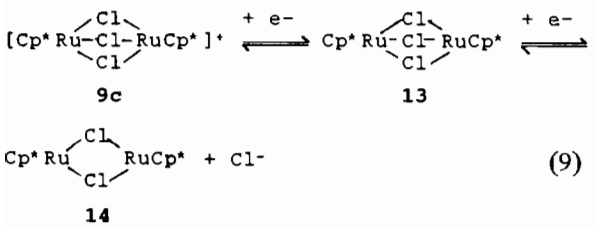

9c **13** **14** (9)

The reversibility of the second step strongly suggests that also the Ru(II) halide under these conditions persists as a dimer, possibly as a methanol solvate. Complex **14** has been found to be stable in MeOH [1].

More complicated are the cyclic voltammograms in CH_2Cl_2 and in THF. In neither solvent is the Ru(II) complex **14** chemically stable. The isolated compound has been found to undergo rapid reaction with CH_2Cl_2 as well as with THF. In CH_2Cl_2 the development of a green solution indicated the formation of the mixed valence complex **13** (oxidative addition of the solvent followed by reaction (11) is a straightforward explanation); in THF a brown complex of yet unknown composition is formed. Therefore the reduction must be chemically irreversible in both steps.

As can be seen from Figs. 9 and 10 a two step reduction is seen also in these solvents. In CH_2Cl_2 the two steps are very close together and separable only at slow scan rates. In THF they are slightly more separated. Whereas the first step seems totally irreversible, the second has some reversibility even at ν = 20 mV/s. The anodic return gives mainly two peaks in CH_2Cl_2 and one peak in THF. Extending the cathodic sweep to more negative potentials reveals a second irreversible reduction with follow up peaks largely the same as those observed for the less negative sweeps.

The cyclovoltammetric behavior is assigned to the sequence eqns. (10) to (12) on the basis of the following arguments taken from observations made in THF solution but pertaining to CH_2Cl_2 with minor modifications.

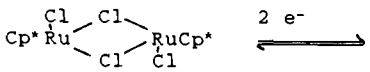

$$\text{Cp}^*\text{Ru}(\mu\text{-Cl})_2\text{RuCp}^* + 2\ e^- \rightleftharpoons$$

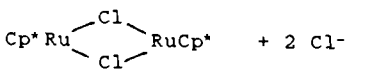

$$\text{Cp}^*\text{Ru}(\mu\text{-Cl})_2\text{RuCp}^* + 2\ \text{Cl}^- \qquad (10)$$

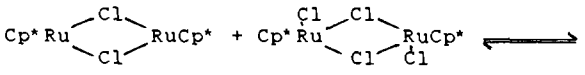

$$\text{Cp}^*\text{Ru}(\mu\text{-Cl})_2\text{RuCp}^* + \text{Cp}^*\text{Ru}(\mu\text{-Cl})_2\text{RuCp}^* \rightleftharpoons$$

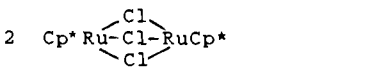

$$2\ \text{Cp}^*\text{Ru}(\mu\text{-Cl})_3\text{RuCp}^* \qquad (11)$$

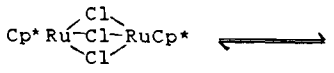

$$\text{Cp}^*\text{Ru}(\mu\text{-Cl})_3\text{RuCp}^* \rightleftharpoons$$

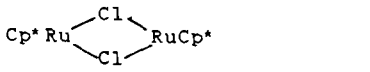

$$\text{Cp}^*\text{Ru}(\mu\text{-Cl})_2\text{RuCp}^* \qquad (12)$$

(i) The peak currents do not follow an inverse $\sqrt{\nu}$-relation ($i/\sqrt{\nu}$ being 1.8 at $\nu = 20$ and 1.5 at $\nu = 500$ for **9** in CH_2Cl_2) indicating kinetic control of the current.

(ii) There is a marked dependence of the cyclic voltammetric pattern on the bulk concentration: at low concentration (5×10^{-4} M) the two reduction peaks of Fig. 10 are of low intensity as compared to the second reduction at more negative potential (around -1 V in THF). At higher concentration (2×10^{-3} M) both steps approach an intensity ratio of 1:1.

(iii) Observation made on electrolysis.

Since the whole pattern is obviously kinetically determined it is concluded that in fact the first reduction is bielectronic (referred to a binuclear complex) and leads directly to the Ru(II) halide **14**. This latter rapidly reacts with the starting complex in a symproportionation, eqn. (11), forming the mixed valence species as a follow up product. The dip in the cyclic voltammogram then marks the onset of this catalytic reaction.

Equation (11) has been proven chemically by reacting together **9** and **14** and electrochemically by electrolyzing the solution on the plateau of the reduction, which after passage of 0.5 F/Ru afforded the green solution characteristic for the formation of **14**. Scanning the cyclic voltammogram at this composition shows the oxidation peak at 0.47 V to be present at a pure anodic scan. It is thus assigned the oxidation of the mixed valence complex **13**.

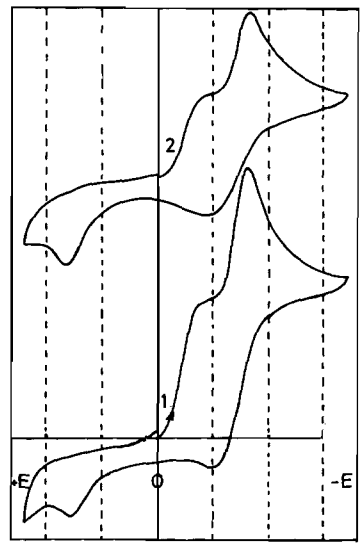

Fig. 9. Cyclic voltammogram of $[Cp^*RuCl_2]_2$ (**9**) in THF/0.1 M TBAH. 1: ν = 20 mV/s, 2: ν = 100 mV/s.

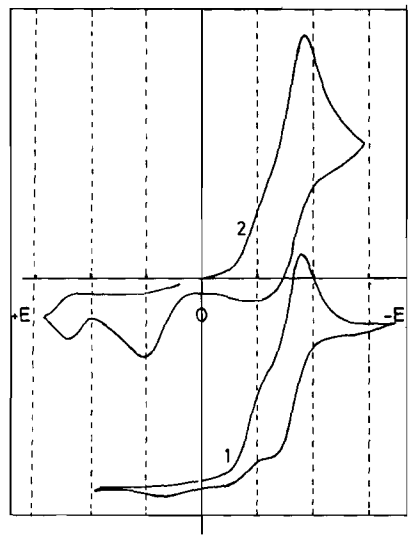

Fig. 10. Cyclic voltammogram of $[Cp^*RuCl_2]_2$ (**9**) in CH_2Cl_2/0.1 M TBAH. 1: ν = 20 mV/s, 2: ν = 100 mV/s.

Most interestingly as is shown in Fig. 11, the inflexion in the cathodic scan has now largely disappeared. On consecutive cycles it reappears once a cathodic/anodic cycle has been completed. Likewise the dip is present if the scan is started anodically. That means sweeping through the anodic peak at 0.47 V regenerates the Ru(III)/(III) complex near the electrode allowing reaction (11) to occur again.

Electrolysis beyond 0.5 F finally yields a dark brown solution, which is no longer air sensitive

and has an oxidation peak at 0.77 V. This peak is also present as one of the follow up peaks after a reductive sweep extended to very negative potentials. The peak at negative potential (−1 V) is therefore ascribed to the reduction of complexes that follow from the reaction of **14** with the solvent and are considered a Ru(III) to a Ru(II) rather than a Ru(II) to Ru(I) reduction. Consistently the oxidation peak at 0.77 V appearing after electrolysis pertains to the oxidation of the reaction product of **14** with the solvent THF and is assigned, in agreement with the potential range where it appears, a Ru(III)/Ru(IV) oxidation.

From the two anodic follow up peaks in the cyclic voltammogram in CH_2Cl_2 the second one is similarly assigned to the reoxidation of **13** whereas the first is due to a transient intermediate (**14**?), since it is relatively more intense at faster scans. Note that this interpretation implies that the onset of the Ru(III)/(III) to Ru(II)/(II) reduction is at more positive potential than the reduction of Ru(III)/(III) to Ru(III)/(II). On the other hand, since the former is coupled to either reaction (11) or to the reaction with the solvent its true potential is difficult to estimate.

In summary the electrochemistry of **9** in CH_2Cl_2 and THF at an inert electrode consists of a sequence of reductions of the binuclear complexes originally present in solution, which react either with excess starting complex or with the solvent depending on the concentration of the former in the reaction layer. The reversibility of both reduction peaks in MeOH as opposed to CH_2Cl_2 and THF is due to the greater stability of **14** in this solvent on the one hand and, as far as the reversible reduction/oxidation of **13** is concerned to the stabilization of the ionic form **9b**, the electron transfer product of **13**, in the more polar solvent.

A pure anodic scan of **9** in CH_2Cl_2 shows an irreversible oxidation peak at 0.81 V followed by a broad reduction at 0.4 V which must be assigned oxidation to some Ru(IV) complex of the type Cp^*RuCl_3 as described by Suzuki *et al.* [5].

A further change in the cyclic voltammograms occurs if the latter are run in the presence of excess Cl^- ion, i.e. using benzyltriethylammoniumchloride as the supporting electrolyte. As seen from Fig. 12 a single reduction peak and a single oxidation peak, both independent from one another and both irreversible at all sweep rates occur in CH_2Cl_2. Both peak potentials are, at comparable sweep rates, shifted cathodic with respect to the solution not containing excess Cl^-, well compatible with the fact that reduction is associated with loss and oxidation with uptake of Cl^-. We do not have at present a ready explanation for the fact why under these circumstances no follow up products are seen in the cyclic voltammogram.

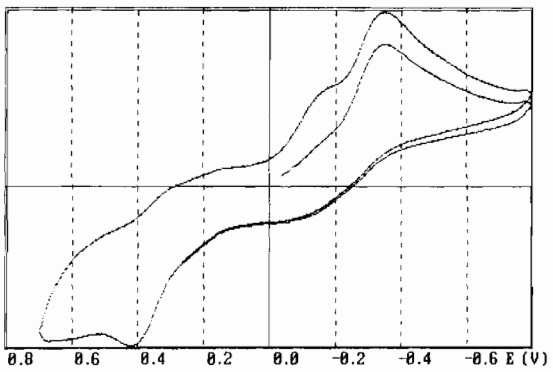

Fig. 11. Cyclic voltammogram of $[Cp^*RuCl_2]_2$ (**9**) in THF/0.1 M TBAH after passage of 0.5 F, ν = 200 mV/s. First cathodic sweep is devoid of the inflection at −0.18 mV, see text.

Still different is the behavior in THF in the presence of excess Cl^- added in the form of anhydrous LiCl. A change in color and greatly enhanced solubility along with a shift of the Cp* signal in the ^1H NMR spectrum from δ 2.42 to 9.9 with excessive broadening indicates the formation of a different species, assigned the structure of a mononuclear LiCl addition product $[Cp^*RuCl_3]Li$ on the basis of its NMR displacement. This now undergoes a quasireversible oxidation/reduction, Fig. 13, at slow scan rates. Close inspection of the cyclic voltammogram at different scan rates shows the reduction to proceed faster than the reoxidation. In this case there is no further reduction prior to the solvent, thus the Ru(II) complex must be stabilized too by the LiCl. Again the oxidation due to the Ru(III)/(IV) transition, which is not very well developed

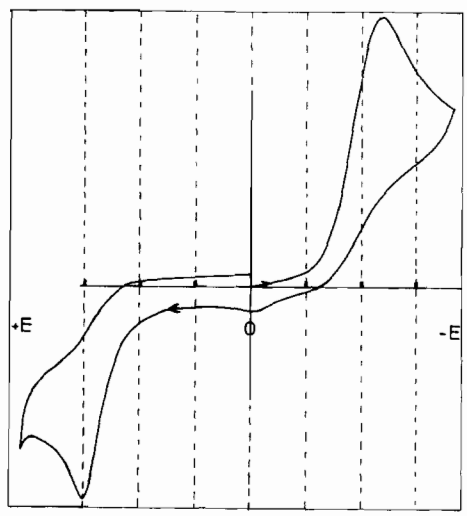

Fig. 12. Cyclic voltammogram of $[Cp^*RuCl_2]_2$ (**9**) in CH_2Cl_2/0.1 M TEBACl; ν = 100 mV/s.

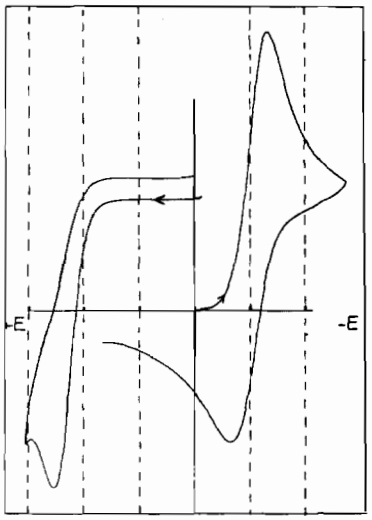

Fig. 13. Cyclic voltammogram of $[Cp^*RuCl_2]_2$ (**9**) in THF/0.1 M LiCl; ν = 100 mV/s.

in the TBAH electrolyte now occurs as a distinct peak at 0.5 V considerably cathodic from its previous value.

Halogeno complexes **10** and **11** were only studied in CH_2Cl_2. The general pattern is similar to the one observed for **9** and is exemplified in Fig. 14 for compound **10**. The onset of the reduction is more positive for both halides and the difference between the first and the second peak is much more pronounced, evident not only by the larger potential separation but also by the kinetic behavior.

Distinct peaks are seen at slow scan rates (20 mV/s) only. At faster scan rates (>100 mV/s) the cyclic voltammogram becomes more drawn out, where especially the second peak in the cathodic direction is shifted negative. For complex **11** the cathodic part of the cyclic voltammogram is a nearly

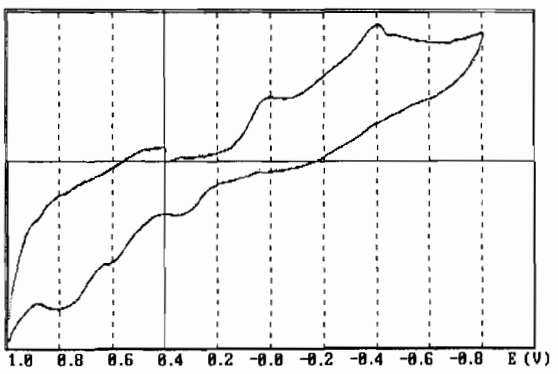

Fig. 14. Cyclic voltammogram of $[Cp^*RuBr_2]_2$ (**10**) in CH_2Cl_2/1 M TBAH; ν = 100 mV/s.

continuous rise in current, distinct peaks are developed only on the anodic sweep.

The difference to **9** is interpreted in terms of slower follow up reactions in particular delayed loss of halide ion on electron uptake making the catalytic reactions slow on the electroanalytical timescale.

From the two anodic peaks the first one with E_p = 0.435 V is assigned to the oxidation of the mixed valence species and the second one with E_p = 0.725 V to a Ru(III)/(IV) transition since it is present also on a mere anodic sweep.

Conclusions

Cp*Ru halfsandwich complexes in general show an involved redox chemistry. Simple electron transfer is encountered only in cases where the cationic complexes $[Cp^*RuL_2X]^+$ are stabilized by strong acceptor or reasonable donor–acceptor ligands. The associated redox potential follows the donor–acceptor properties of L as is demonstrated for the series COD, PR_3, bipyridine with complexes **4**, **1** and **3**.

The reduction of Ru(III) complexes Cp^*RuLX_2 is generally accompanied by loss of halide and uptake of additional ligand L if present in solution. In this way Ru(II) complexes Cp^*RuL_2X with simple donor ligands like pyridine or acetonitrile, which are not readily isolable compounds, are formed as intermediates. Since in these cases L does not stabilize the cation $[Cp^*RuL_2X]^+$, oxidation regenerates the starting complex Cp^*RuLX_2, leading to an overall ECEC electrochemical reaction scheme.

Electrochemical reduction of halogeno complexes $[Cp^*RuX_2]_2$ is even more complicated due to the comproportionation of Ru(II) and Ru(III) to a mixed valence dinuclear complex and the reaction of the Cp*Ru(II) halide with the solvent if this latter was CH_2Cl_2 or THF.

The typical potential range where oxidation/reduction between the Cp*Ru(II)/Ru(III) valence states occurs can be stated as −0.5 to 0.5 V versus SCE in the organic solvents. An oxidation assigned to a Ru(III)/Ru(IV) transition is seen frequently in the potential range 0.5–0.8 V. Of particular interest seems the observation of a catalytic wave for **9** in the presence of methanol at the relatively mild potential of about 0.7 V versus SCE. Similarly important is the reduction of **9** in methanol at about 0 V versus SCE since it has been found [1] that methanol, as well as other primary and secondary alcohols, is capable of reducing **9** to the Ru(II) complex $[Cp^*RuOR]_2$ in a stoichiometric reaction at room temperature. The significance of these latter observations on catalytic alcohol oxidation is presently under study in our laboratory.

Acknowledgements

Support by the Deutsche Forschungsgemeinschaft (to J.K.) and by the Fonds der Chemischen Industrie as well as a gift of $RuCl_3$ from Degussa AG, Hanau, is gratefully acknowledged.

References

1 (a) U. Koelle and J. Kossakowski, *J. Organomet. Chem., 362* (1989) 383; (b) U. Koelle and J. Kossakowski, *J. Chem. Soc., Chem. Commun.*, (1988) 459.
2 (a) T. Don Tilley, R. H. Grubbs and J. E. Bercaw, *Organometallics, 3* (1984) 274; (b) N. Oshima, H. Suzuki and Y. Moro-oka, *Chem. Lett.*, (1984) 1161.
3 (a) M. I. Bruce, in G. Wilkinson and E. Abel (eds.), *Comprehensive Organometallic Chemistry*, Vol. 4, Pergamon, Oxford, 1982, pp. 661–690; (b) M. A. Bennett, M. I. Bruce and T. W. Matheson, pp. 691–841.
4 (a) H. Nagashima, K. Yamagushi, K. Mukai and K. Itoh, *J. Organomet. Chem., 291* (1985) C20; (b) T. Arliguie and B. Chaudret, *J. Chem. Soc., Chem. Commun.*, (1986) 985; (c) M. Hidai, K. Imagawa, G. Cheng, Y. Mizobe, Y. Wakatsuki and H. Yamazaki, *Chem. Lett.*, (1986) 1299.
5 (a) N. Oshima, H. Suzuki, Y. Moro-oka, H. Nagashima and K. Itoh, *J. Organomet. Chem., 314* (1986) C46; (b) H. Suzuki, D. H. Lee, N. Oshima and Y. Moro-oka, *Organometallics, 6* (1987) 1569; (c) H. Nagashima, K. I. Ara, K. Yamagushi and K. Itoh, *J. Organomet. Chem., 319* (1978) C11; (d) A. Efraty and G. Elbaze, *J. Organomet. Chem., 260* (1984) 331; (e) M. I. Bruce, *J. Chem. Soc., Dalton Trans.*, (1982) 687; (f) C. White, *J. Chem. Soc., Chem. Commun.*, (1979) 547.
6 (a) K.-Y. Wong, C.-M. Che and F. C. Anson, *Inorg. Chem., 26* (1987) 731; (b) B. A. Moyer, M. S. Thompson and J. T. Meyer, *J. Am. Chem. Soc., 102* (1980) 2310; (c) C.-M. Che, W.-H. Leung and C.-K. Poon, *J. Chem. Soc., Chem. Commun.*, (1987) 173.
7 M. Grätzel (ed.), *Energy Resources Through Photochemistry and Catalysis*, Academic Press, New York, 1983; R. Ramaraj, A. Kira and M. Kaneko, *Angew. Chem., 98* (1986) 1012, and refs. therein.
8 E. A. Seddon and K. R. Seddon, *The Chemistry of Ruthenium*, Elsevier, Amsterdam, 1984.
9 J. C. Cyr, J. A. DeGray, D. K. Gosser, E. S. Lee and P. H. Rieger, *Organometallics, 4* (1985) 950.
10 W. E. Geiger and N. Connelly, *Adv. Organomet. Chem., 23* (1984) 2; *24* (1985) 87.

Note Added in Proof

$Cp^*Ru(acac)PPh_3$ has meanwhile been prepared and characterized in our laboratory.